Study on Sensitivity of Ship Added Resistance to Wave Slope

Byung-Soo Kim[1], Kyung-Kyu Yang[2] and Yonghwan Kim[1]*

[1] Department of Naval Architecture and Ocean Engineering, Seoul National University, Seoul, Korea

[2] Korea Research Institute of Ships & Ocean Engineering, Daejeon, Korea

*yhwankim@snu.ac.kr

1 INTRODUCTION

Ship added resistance, which is additional resistance when ship travels in waves, is one of the key fields to be studied as International Maritime Organizations (IMO) started to regulate Energy Efficiency Design Index (EEDI) for large ships. In order to reduce the ship added resistance, it is important to understand physical phenomena and main source of resistance increase in waves.

From the past, many studies have been carried out and it was treated that added resistance is proportional to the square of wave amplitude by both theoretically and experimentally. Some recent studies show that added resistance is a stronger nonlinear phenomenon which depends on the ship hull shape and the wave slope. In this study, the effect of wave height on ship added resistance is studied using a nonlinear Cartesian-grid-based solver, particularly for harsh conditions to do experiments.

2 COMPUTATIONAL METHOD

2.1 Computational Solver

Cartesian based method, SNU-MHL-CFD (Yang et al., 2015), was used for the calculation. In this computation, Euler equation is solved based on a Cartesian grid method. Governing equations are as follows:

$$\int_{\Gamma} (\vec{u} \cdot \vec{n})\, dS = 0 \tag{1}$$

$$\int_{\Omega} \frac{\partial \vec{u}}{\partial t} dV = -\int_{\Gamma} u(u \cdot n)\, dS + \frac{1}{\rho}\left[-\int_{\Gamma} p\vec{n} dS + \int_{\Omega} \vec{f}_b dS \right] \tag{2}$$

Pressure-velocity coupling problem is solved by a fractional step method. In each cell, volume fraction of water, air and body is obtained, and the free surface is obtained as a result of solving transport equations on water. Level-set method was used to simulate the body hull and immersed boundary method was used to solve the ship motion. To generate and damp the wave, forcing method was used at the inlet, outlet and side boundaries. More details of Cartesian-grid-based method can be found in Yang et al. (2015).

2.2 Ship Model

This paper introduces the results for the S-LNGC (Samsung Heavy Industries' Liquefied Natural Gas Carrier) model. This ship model is a modern large LNG carrier which has twin-skeg hull with bulbous bow(Kim et al., 2017). Its ship speed has the Froude number of 0.188. Fig. 1 shows the ship model tested at towing tank.

Fig. 1 Ship model: S-LNGC

2.3 Numerical Tank

Numerical tank is generated based on Cartesian type mesh. As calculation models are symmetry with respect to the breadth direction, only the half of the domain was generated. The domain size was determined by wavelength and near the bow and stern, meshes are refined to capture the bow waves and stern flows better. Because the mesh system is also an important factor to generate better wave profiles, more than 75 meshes were used per wavelength ($\lambda/\Delta x \geq 75$) and more than 10 meshes were used per wave height ($H/\Delta z \geq 10$. Also, aspect ratio was selected to be less than 20 ($\Delta x/\Delta z \leq 20$). Example of Cartesian-grid is shown in Fig. 2.

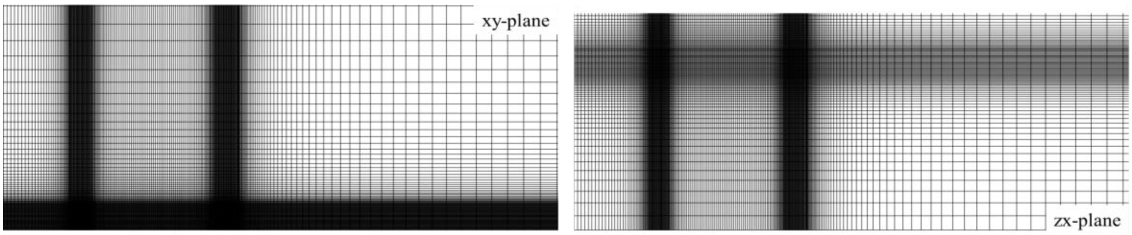

Fig. 2 Example of numerical tank used for the calculation

3 CALCULATION RESULTS

In this numerical computation, motion responses and added resistance for different wavelengths are first calculated and then wave slope is changed between 1/40 and 1/25 for fixed wavelengths: short wavelength (λ/L = 0.4) and wavelength near the resonance (λ/L = 1.0). Test cases are also summarized in table 1. Computed results are compared to the experiments conducted in Seoul National University Towing Tank (Lee and Kim, 2017).

Table 1 Test matrix for added resistance calculation for different wave amplitude

λ/L	0.4			1.0		
H/λ	0.025	0.033	0.040	0.025	0.033	0.040
kA	0.079	0.105	0.126	0.079	0.105	0.126

A summary of calculation results are shown in Fig. 3. Computed results matched well with the experiments conducted under the same wave slope condition. Note that, for more severe wave slope condition, experiments cannot be conducted properly due to large nonlinear phenomenon like green water or exposure of bulbous bows. From the experiments, although the heave motion slightly decreased as wave slope changes, the drastic reduction of added resistance is resulted: which can be interpreted as nonlinear phenomenon of added resistance.

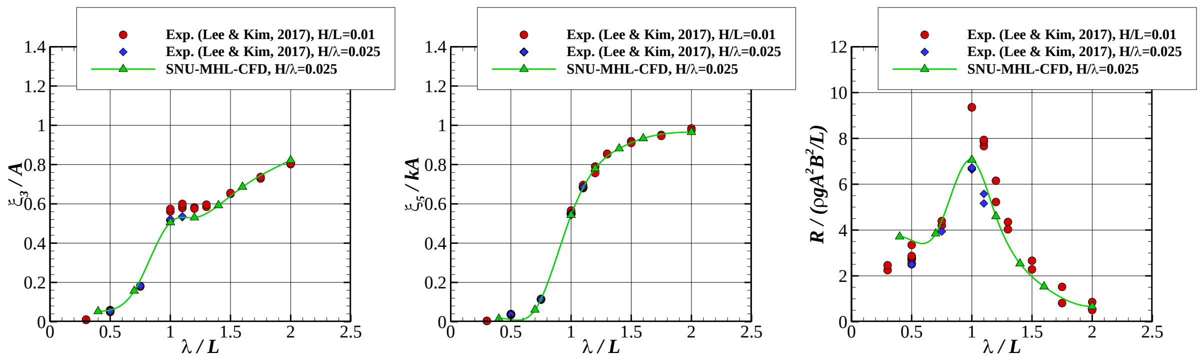

(a) Heave motion (b) Pitch motion (c) Added resistance

Fig. 3 Motion responses and added resistance of S-LNGC (*Fn* = 0.188, head sea)

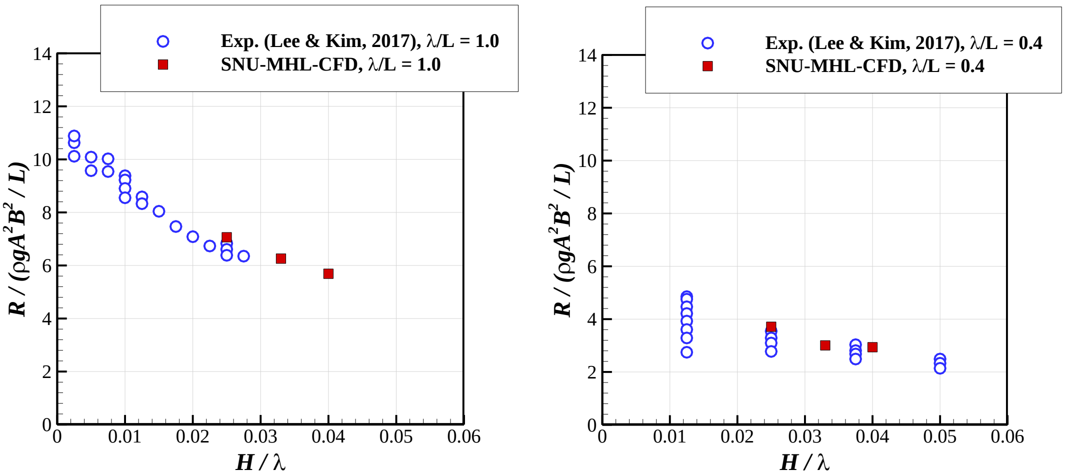

(a) $\lambda/L = 1.0$ (b) $\lambda/L = 0.4$

Fig. 4 Added resistance of S-LNGC for different wave slope (*Fn* = 0.188, head sea)

Fig. 4 shows the change of added resistance of S-LNGC due to the wave slope change. At the resonance frequency, as the wave height increases, obtained added resistance became smaller. Estimated results followed similar trend with the experiments. For the short wavelength, obtained added resistance were within the experimental data and did not show significant change compared to the results at resonance frequency. This phenomenon conflicts with the previous studies that ship added resistance is proportional to amplitude square. Due to nonlinear hull shapes including bulbous bow and large flare angle, it could be inferred that wetted surface area might not be proportional to wave amplitude which can be cause of the nonlinearity.

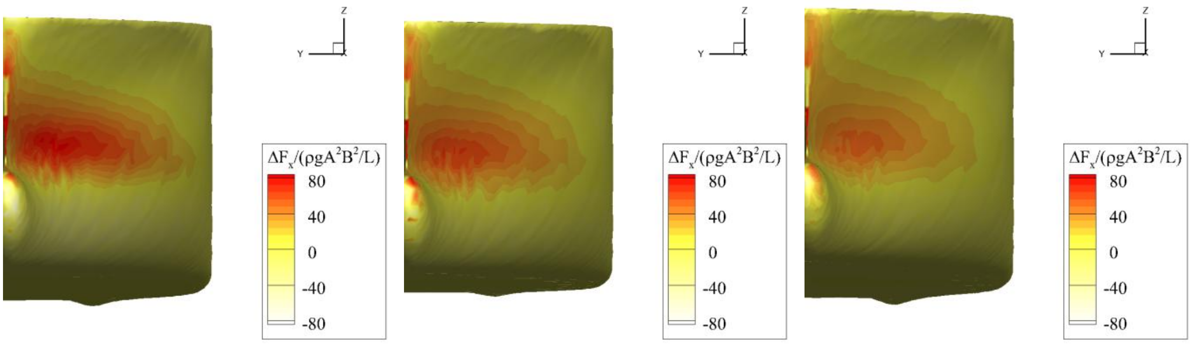

(a) $H/\lambda = 0.025$ (b) $H/\lambda = 0.033$ (c) $H/\lambda = 0.040$

Fig. 5 Added force contours of S-LNGC for different wave slope (*Fn* = 0.188, head sea, *λ*/*L* = 1.0)

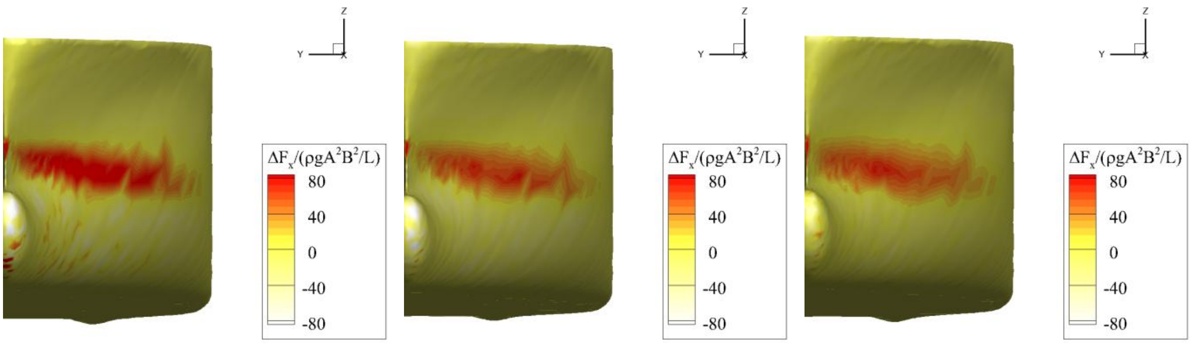

(a) $H/\lambda = 0.025$ (b) $H/\lambda = 0.033$ (c) $H/\lambda = 0.040$

Fig. 6 Added force contours of S-LNGC for different wave slope (*Fn* = 0.188, head sea, *λ*/*L* = 0.4)

To understand the reduction of added resistance when ship encounters higher waves, pressure distribution over ship surface was analyzed. Because the pressure obtained from the simulation (p_{us}) is unsteady, pressure was time averaged and to eliminate the static pressure, pressure from the steady state calculation (p_s) was subtracted to obtain added pressure (p_{add}). However, using pressure distribution only would be valid when ship encounters short waves where ship motions are almost negligible. When ship experiences resonance, relative ship motion would be large and change of surface normal vectors needed to be considered. Moreover, pressure obtained from equation (3) includes not only pressure in *x*-direction, but also in *y*- and *z*-directions. In order to ignore the effects in other directions, *x*-direction normal vector (n_x) was multiplied to the pressure and the added force (ΔF_x) is obtained as in equation (4).

$$p_{add} = \overline{p_{us}} - p_s \tag{3}$$

$$\Delta F_x = p_{add} n_x = \overline{p_{us} n_x} - p_s n_x \tag{4}$$

Added forces are normalized by amplitude square same as the typical wave to normalize added resistance. In Figs. 5 and 6, normalized added forces for resonance wavelength and short wavelength are plotted respectively to observe the nonlinear effect. In Fig. 5, the results show that for smaller wave amplitude, normalized added forces are bigger compare to that of bigger wave amplitude. This is contrary to the linear theories where added resistance is proportional to wave amplitude square. Also, the region for the added forces is diminished. This corresponds to the previous results that ship added resistance reduced as the wave amplitude increased. Short wavelength showed no significant change in added force, although slightly bigger added force can be seen for the small wave steepness. Comparing the results for the same wave slope, added forcing area was larger in resonance due to bigger wave height whereas negative added force area was larger in short waves. Consequently, ship experiences more added resistance in resonance wavelength rather than in short wavelength.

4 CONCLUSIONS

Following conclusions can be made based on this study:

- Motion responses and added resistance obtained using the present Cartesian-grid-based method showed similar values to the experimental data.
- Near the resonance frequency, as the wave slope increase, the added resistance tends to reduce which matches well with the experiments. For short wavelengths, the added resistance was less sensitive to the wave slope.
- The normalized added force is reduced near resonance, while not much difference is shown in short wave cases.

ACKNOWLEDGEMENT

This study was supported by the Ministry of Trade, Industry and Energy (MOTIE), Korea, through the project number 10062881, “Technology Development to Improve Added Resistance and Ship Operational Efficiency for Hull Form Design”. Their supports are appreciated. Moreover, supports from the Lloyd’s Register Foundation (LRF)-Funded Research Center at Seoul National University are also respected.

REFERENCES

Kim, T.Y. et al., 2017. Numerical and Experimental Study on the Estimation of Added Resistance of an LNG Carrier in Waves. *Proc. 27th ISOPE*, San Francisco, California, USA

Lee, J. & Kim, Y., 2017. Study on the effect of wave amplitude on added resistance. *Proc. Annual Autumn Conference, SNAK*, Yeosu, Korea

Yang, K.-K. et al., 2015. Cartesian-grid-based computational analysis for added resistance in waves, *J Mar Sci Technol*, 20, 155-170